This is an open access article published under a Creative Commons Non-Commercial No Derivative Works (CC-BY-NC-ND) Attribution License, which permits copying and redistribution of the article, and creation of adaptations, all for non-commercial purposes.

ACS AuthorChoice

ACS APPLIED MATERIALS & INTERFACES

Research Article

www.acsami.org

Enabling Ambipolar to Heavy n-Type Transport in PbS Quantum Dot Solids through Doping with Organic Molecules

Mohamad Insan Nugraha,[†,‡,#] Shohei Kumagai,[‡,#] Shun Watanabe,[‡,§] Mykhailo Sytnyk,[∥,⊥] Wolfgang Heiss,[∥,⊥] Maria Antonietta Loi,[*,†] and Jun Takeya[*,‡]

[†]Zernike Institute for Advanced Materials, University of Groningen, Nijenborgh 4, Groningen 9747AG, The Netherlands

[‡]Department of Advanced Materials Science, School of Frontier Sciences, The University of Tokyo, 5-1-5 Kashiwanoha, Kashiwa, Chiba 277-8561, Japan

[§]JST, PRESTO, 4-1-8 Honcho, Kawaguchi, Saitama 332-0012, Japan

[∥]Materials for Electronics and Energy Technology (i-MEET), Friedrich-Alexander-Universität Erlangen-Nürnberg, Martensstraße 7, 91058 Erlangen, Germany

[⊥]Energie Campus Nürnberg (EnCN), Fürther Straße 250, 90429 Nürnberg, Germany

Supporting Information

ABSTRACT: PbS quantum dots (QDs) are remarkable semiconducting materials, which are compatible with low-cost solution-processed electronic device fabrication. Understanding the doping of these materials is one of the great research interests, as it is a necessary step to improve the device performance as well as to enhance the applicability of this system for diverse optoelectronic applications. Here, we report the efficient doping of the PbS QD films with the use of solution-processable organic molecules. By engineering the energy levels of the donor molecules and the PbS QDs through the use of different cross-linking ligands, we are able to control the characteristics of PbS field-effect transistors (FETs) from ambipolar to strongly n-type. Because the doping promotes trap filling, the charge carrier mobility is improved up to 0.64 $cm^2 V^{-1} s^{-1}$, which is the highest mobility reported for low-temperature processed PbS FETs employing SiO_2 as the gate dielectric. The doping also reduces the contact resistance of the devices, which can also explain the origin of the increased mobility.

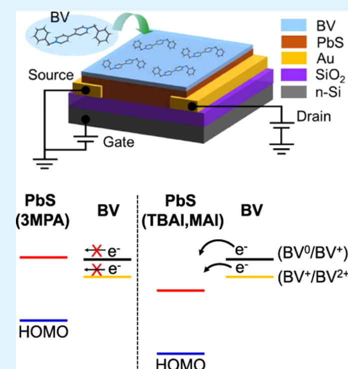

KEYWORDS: *quantum dots, benzyl viologen, doping, ligands, field-effect transistors*

INTRODUCTION

PbS colloidal quantum dots (QDs) have been shown to be promising as semiconducting building blocks for optoelectronic devices, such as solar cells,[1−7] photodetectors,[8−11] and light-emitting devices.[12−14] This class of materials makes it possible to fabricate electronic devices using solution-processable methods such as blade-coating, dip-coating, printing, and roll-to-roll processes.[15−20] Recently, many efforts have been devoted to exploit PbS QDs as active materials for field-effect transistors (FETs).[17,18,21,22] The fabrication of FETs offers the possibility to integrate them in more advanced electronic devices, such as complementary metal oxide semiconductor-like inverters, integrated logic circuits, radio frequency identification systems, etc.[23,24] Their use in FETs, however, is still challenging because they suffer from low charge carrier mobility due to the high number of carrier traps on their surface. Therefore, improving the charge carrier mobility in FETs based on PbS QDs is crucial to enhance their potential for diverse applications.

Doping is an effective tool to improve the charge carrier mobility in semiconductors.[24−27] Although PbS QDs are n-type on the basis of their stoichiometry,[5,22,28] many published studies show strategies to turn them into p-type.[29,30] The p-type doping is mainly achieved by exposing samples to air, which gives rise to a significant increase of the hole mobility and density in the films.[29,30] A better control was achieved by evaporation of sulfur and selenium, or acting on the surface of the QDs with specific ligands.[5,22,31] On the other hand, studies on heavy n-type doping of the PbS QD films are still limited. The energy offset often built at the interface of semiconductor and dopant is responsible for inefficient electron transfer from the highest occupied molecular orbital (HOMO) of the dopant to the lowest unoccupied molecular orbital (LUMO) of the semiconductor.[32] Recently, benzyl viologen (BV) has been reported as a promising n-type dopant for the carbon nanotubes and MoS_2 systems.[26,33] Due to its shallow HOMO level, BV molecule treatment induces carrier doping in samples which favors electron transfer to the semiconducting films. To date, the use of BV as an n-type dopant in PbS QD films has not been investigated yet. This leaves a question on the possibility to use BV for obtaining strong n-type doping of the

Received: February 27, 2017
Accepted: May 5, 2017
Published: May 5, 2017

© 2017 American Chemical Society

DOI: 10.1021/acsami.7b02867
ACS Appl. Mater. Interfaces 2017, 9, 18039−18045

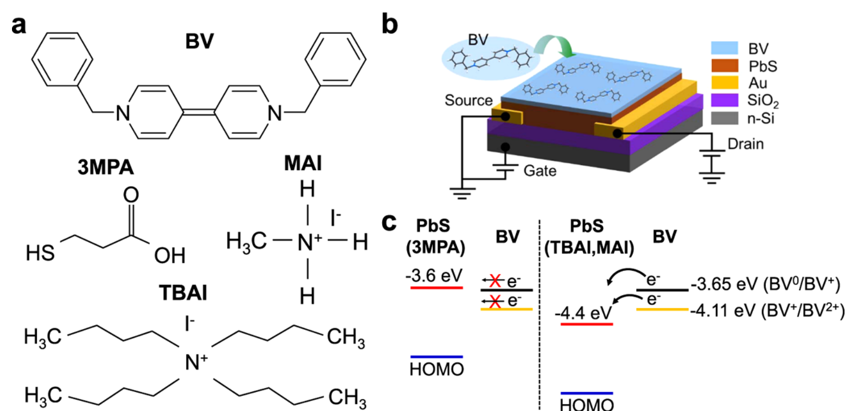

Figure 1. (a) Chemical structure of the BV molecules and the capping ligands used in this study, (b) device structure, and (c) schematic of the electron transfer mechanism from BV to PbS QDs, with different capping ligands. After transferring an electron, BV^0 (black) turns to BV^+ state (orange), with deeper HOMO level.

PbS films and improving the performance of FET devices based on these QDs.

Here, we report a strategy for doping PbS QD solids using BV as the donor molecules. By combining the use of BV with engineering of the QD energy levels through the use of several capping ligands, we are able to effectively tune the electrical properties of the PbS QD-FETs from ambipolar to heavily n-type. With this BV treatment, we improve the electron mobility by 1 order of magnitude and we reduce the contact resistance down to 0.77 kΩ cm. Furthermore, the four-terminal (4T) conductivity transistor measurements confirm the efficient doping of the PbS QD films after BV treatment leading to electron mobility as high as 0.64 $cm^2\ V^{-1}\ s^{-1}$, the highest value reported for the low-temperature processed PbS QD-FETs employing a SiO_2 gate dielectric.

EXPERIMENTAL DETAILS

Material Preparation. PbS colloidal QDs 3.6 nm in diameter were synthesized by following a previously reported method.[40,41] For ligand exchange (LE), we used three kinds of molecules, namely, 3-mercaptopropionic acid (3MPA), tetrabutylammonium iodide (TBAI), and methylammonium iodide (MAI). 3MPA ligand solution was prepared by dissolving 3MPA in methanol (115 mM). TBAI and MAI powders were dissolved in methanol (30 mM) to form TBAI and MAI ligand solutions, respectively. The solutions were then filtered by poly(tetrafluoroethylene) filter (0.45 μm) before use.

The BV solution was prepared according to previous reports with some modifications for use in glovebox.[26,33] In distilled water (4.5 mL) inside a vial, 51 mg (0.12 mmol) of 1,1′-dibenzyl-4,4′-bipyridinium dichloride hydrate was dissolved. Toluene (9.0 mL) was carefully layered on the aqueous layer, and 97 mg (2.5 mmol) of $NaBH_4$ was added into the bilayer system. The colorless aqueous layer immediately started to turn into deep violet with the generation of hydrogen gas. After 12 h, the aqueous layer turned colorless and the top toluene layer became yellow. The toluene layer was separated and dried over $MgSO_4$ and filtered into a glass Schlenck flask. The solvent was removed under vacuum and heating, and then dry hexane/toluene (1:1 (v/v); 32 mL) was added into the yellow oily residue, affording a yellow solution. The BV solution was transferred into a glovebox after argon bubbling for 15 min.

Device Fabrication. We used SiO_2/n-Si substrates with lithographically defined prepatterned interdigitated Au electrodes. The thickness of the SiO_2 dielectric was 230 nm. The channel length and width of the devices were 20 μm and 1 cm, respectively. Before use, the substrates were cleaned with acetone and isopropanol using ultrasonicator for 10 min. The substrates were then dried at 120 °C for 10 min to remove residual organic solvents.

On the clean substrates, PbS films were then deposited by spin-coating the oleic acid-stabilized PbS solution in chloroform (10 mg/mL). To improve the conductivity of the films, the long oleic acid ligands were replaced by shorter molecules or halide atoms. The deposition of semiconducting thin film and LE were performed layer-by-layer seven times to ensure complete LE process. For LE, the ligand solution was dropped onto the previously deposited oleic acid-capped PbS films for 30 s and then spin-casted for 60 s. After each LE process, pure methanol was dropped for another 30 s and then spin-casted for 60 s to remove native oleic acid ligands. The devices were then annealed at 120 °C for 20 min to remove residual solvents and to enhance coupling between QDs. The BV-doping treatment was done by dipping the previously fabricated devices into BV solution for 3 min. The samples were then dried at room temperature under argon atmosphere. All device fabrication was done in glovebox.

For the fabrication of 4T FETs, we used bare SiO_2/n-Si substrates. Before use, the substrates were cleaned following the cleaning procedure mentioned above. As a source−drain electrode, thermally grown bottom contact Au (30 nm), with Cr (10 nm) as the buffer layer was patterned using a 4T transistor shadow mask. The deposition of the PbS semiconducting thin films, LE, and BV-doping treatment were done following the previously mentioned procedures.

Electrical Measurement. The electrical characteristics of the fabricated devices were measured using an Agilent B1500A semiconductor parameter analyzer connected to a probe station in a glovebox.

RESULTS AND DISCUSSION

The successful doping of a semiconductor device is determined by the effective charge transfer from the dopant molecules to the semiconducting films or vice versa. Several methods have been used to introduce efficient doping of the QD films, including mixing a solution of dopants and QDs prior to film deposition, infiltrating a semimetallic material into the active channels, and dipping the deposited semiconducting films into the dopant solution.[23,32,34,35] Among others, the dipping method has been shown to enable highly efficient optoelectronic devices fabricated with heavily doped PbS QD films.[35] Furthermore, this method has also been used on a broad range of semiconductors leading to significant increase of the film conductivity in the fabricated transistors.[26,33,36,37]

To heavily dope the PbS QD films, we treated the semiconducting films with BV donor molecules, which have a redox potential of −0.79 V (BV^0/BV^+) relative to that of the standard hydrogen electrode (SHE).[26,33] This redox potential corresponds to a HOMO level of −3.65 eV with respect to the vacuum level. Kiriya et al. reported that the BV molecules have

DOI: 10.1021/acsami.7b02867
ACS Appl. Mater. Interfaces 2017, 9, 18039−18045

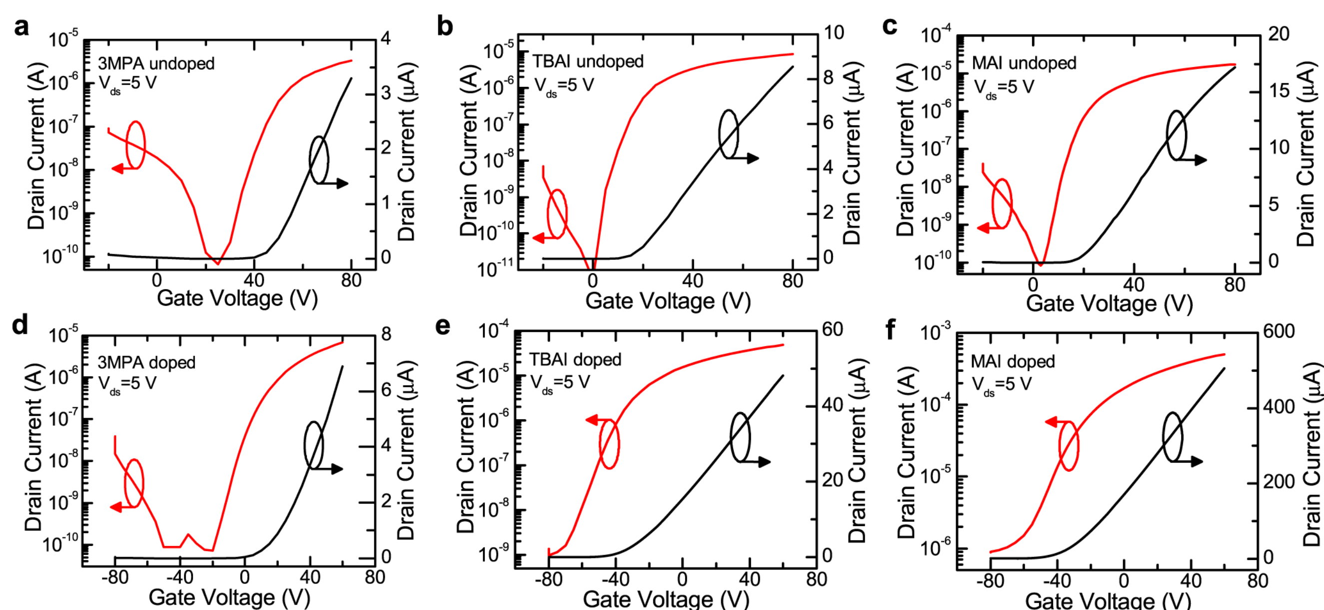

Figure 2. Transfer characteristics of the pristine devices with (a) 3MPA, (b) TBAI, and (c) MAI ligands. Transfer characteristics of the devices with (d) 3MPA, (e) TBAI, and (f) MAI ligands after BV treatment. Transfer characteristics in the linear and semilogarithmic scale are shown in black and red, respectively.

Table 1. Electrical Properties of PbS FETs with Different Capping Ligands before and after BV Treatment

ligands	2T mobility (cm^2 V^{-1} s^{-1}) pristine	2T mobility BV-treated	threshold voltage (V) pristine	threshold voltage BV-treated	doping carrier concentration (10^{12} cm^{-2})
3MPA	2.6×10^{-3}	5.1×10^{-3}	36	18.8	1.6
TBAI	5.3×10^{-3}	1.4×10^{-2}	16.5	−17.1	3.2
MAI	0.03	0.32	12.2	−35	4.4

a second redox potential after releasing an electron, which results in the BV^+ state.[26] In this state, the redox potential (BV^+/BV^{2+}) turns to −0.33 V relative to that of the SHE, which corresponds to a HOMO level of −4.11 eV with respect the vacuum level. The chemical structure of BV is shown in Figure 1a. In this study, doping of the PbS films is done by dipping the deposited films into the BV solution for a specific time. The configuration of the BV-treated PbS QD-FETs is displayed in Figure 1b. To promote the transport of electrons from the dopant to the semiconductor, the LUMO level of the PbS films should be deeper than the HOMO level of the dopant. Recently, it has been reported that the HOMO/LUMO level of PbS QDs is strongly influenced by the cross-linking ligands.[38] Therefore, by varying the ligands, we are able to potentially tune the doping strength of the PbS QD films. Here, we use three kinds of ligands, namely 3MPA, TBAI, and MAI. The chemical structures of the ligands are shown in Figure 1a. These ligands have been reported to enable good performing FET devices based on PbS QDs.[13,15,29] By cross-linking PbS QDs with 3MPA ligands, the LUMO level of the materials is estimated to be around −3.6 and −3.7 eV, which are quite close to the HOMO level of BV.[38] With this energy level offset, some electrons are inefficiently transferred from BV to the PbS films as shown in the schematics of Figure 1c. After releasing an electron, the BV^0 state turns to BV^+ state, which has HOMO of −4.11 eV. This HOMO value is significantly deeper than the LUMO value of 3MPA-capped PbS films, which blocks electron transfer from BV^+ to PbS, leading to an inefficient n-type doping of the PbS films after the BV layer deposition. This unfavorable energy offset could also explain the previously reported inefficient n-type doping of lead chalcogenide films with cobaltocene.[32] With cobaltocene doping, the transport of charge carriers turns to n-type from ambipolar, with a reduced current.

Other types of ligands, such as TBAI and MAI have been reported to result in a deep LUMO level for PbS QDs. The reported LUMO level using this class of ligands is as deep as −4.4 eV.[38] This LUMO level is importantly deeper than both the HOMO levels of BV^0 and of BV^+. Therefore, it opens the possibility to successfully obtain n-type doping in PbS QD films.

The transfer characteristics of the pristine devices (before BV-doping treatment) with different capping ligands are shown in Figure 2a−c. Obviously, the devices show ambipolar properties, with more electron-dominated transport with all of the three ligands. A pronounced difference is observed in the threshold voltages (V_{th}) of the devices. The devices with iodide ligands clearly show smaller V_{th} than those with 3MPA ligands, which indicates a good passivation against carrier traps on the QD surfaces. The lower number of carrier traps in the PbS QD films with iodide ligands than those with 3MPA is also demonstrated by steeper transfer characteristics of the devices in the semilogarithmic scale, as displayed in Figure 2a−c. Meanwhile, in the p-channel characteristics, we also observe a slight hole current. However, in this study, we limit our analysis to the n-type transport because the hole current is much weaker. To estimate the electron mobility (μ) in our devices, we use the following formula for the linear regime

DOI: 10.1021/acsami.7b02867
ACS Appl. Mater. Interfaces 2017, 9, 18039−18045

$$\mu = \frac{L}{WC_iV_{ds}}\frac{\partial I_{ds}}{\partial V_g} \quad (1)$$

where W and L are the channel width and length, respectively, C_i is the capacitance per unit area, V_{ds} is the drain−source voltage, I_{ds} is the drain−source current, and V_g is the gate voltage. Table 1 shows the electron linear mobility in devices with different capping ligands. The standard deviation of the extracted mobility is given in Table S-1. Obviously, the devices with MAI ligands show the highest μ among the other capping ligands, which is comparable to a previous report.[15] The lower μ in the devices with TBAI with respect to the MAI ones is attributed to the presence of the remaining oleic acid ligands on the PbS QD surface, which suppresses charge transport within the QD films. The remaining oleic acid is a result of the poor reactivity of TBAI in the ligand-exchange process due to nonacidity of the cation of TBAI ligands.[15]

The transfer characteristics of the devices after BV treatment are shown in Figure 2d−f. In the devices with 3MPA ligands, we observe that the devices still show the ambipolar characteristics, with a slight increase of the source−drain current (I_{ds}) even after BV-doping treatment, as shown in Figure 2d. The remaining ambipolar properties are explained by our previous hypothesis that an unfavorable offset between the HOMO level of BV and LUMO level of 3MPA-cross-linked PbS QDs leads to a blockade of the electron transfer from the BV layer to the PbS films. Nevertheless, some weak electron transfer from the BV^0 HOMO to the PbS LUMO may result in a shifting of the transfer characteristics to a negative direction, indicating the presence of a certain level of n-type doping. Instead, with TBAI and MAI ligands that enable the shift of the LUMO level of PbS QDs, we observe that the device characteristics turn to heavily n-type from ambipolar after BV-doping treatment, as displayed in Figure 2e,f. In addition, the devices show a normally "on" operation, as indicated by the transfer characteristics on a linear scale, which demonstrates the strong electron doping of the active material.

By analyzing the transfer characteristics further, the devices with MAI ligands show the highest on-current after BV treatment among the other ligands, as given in Figure 3a. The on-current in the MAI-capped PbS FET devices is improved by more than 1 order of magnitude, whereas an improvement by only a factor of 6 is observed in the 3MPA-cross-linked devices after BV treatment. To get a deeper insight into these results, μ in the linear regime is estimated using eq 1. The extracted linear mobility, μ, in all of the fabricated devices, with different ligands before and after BV treatment, is shown in Table 1. In the devices capped with 3MPA ligands, μ is improved only by a factor of 2. Importantly, a significant improvement in μ (the maximum μ is 0.45 $cm^2\ V^{-1}\ s^{-1}$; the average μ is 0.32 $cm^2\ V^{-1}\ s^{-1}$) is observed in the devices with MAI ligands after treatment with BV, indicating a more efficient doping with respect to the case of PbS decorated by the other ligands. The devices with TBAI, which are suggested to have a doping mechanism similar to that of MAI, have a lower increase of μ than that of the devices with MAI. This result can be associated to the more effective removal of oleic acid ligands with MAI than that with TBAI due to the acidity of the methylammonium cation.[15] In addition, among the other ligands, we observe that the BV-doping treatment reduces the bias stress in devices with MAI ligands. This result is supported by the smaller hysteresis observed in devices with MAI after BV treatment with respect to the ones treated with the other ligands, as shown in Figure S1. Therefore, the proper choice of ligands combined with the use of BV results in n-type doping and more stable PbS QD transistors.

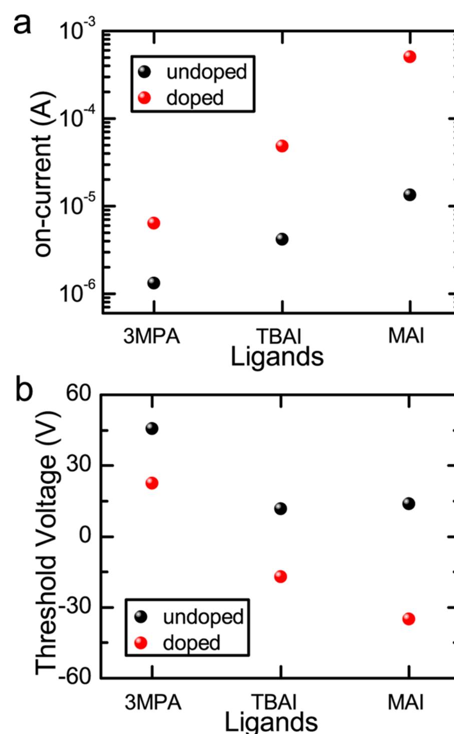

Figure 3. Comparison of (a) on-currents and (b) threshold voltages of the devices before and after BV-doping treatment. The standard deviation of the on-currents and threshold voltages is reported in Figure S2 and Table S-1.

At this point, we are then interested in estimating the doping concentration in devices after BV treatment. The doping concentration in FETs can be calculated by measuring the difference in V_{th} before and after BV treatment ($n_{doping} = C_i\Delta V_{th}/e$) using the following equation in the linear regime.

$$I_{ds} = \frac{\mu C_i W V_{ds}}{L}\left(V_g - V_{th} - \frac{V_{ds}}{2}\right) \quad (2)$$

Using eq 2, we obtain the V_{th} of the devices (with different capping ligands), as given in Table 1. All devices show n-type doping, indicated by the shifting of V_{th} into the negative direction, as displayed in Figure 3b. The doping concentration in all fabricated devices is shown in Table 1. The highest doping concentration is achieved in the devices with the MAI ligands after BV treatment and is estimated to be about 4.4×10^{12} cm^{-2}, which is comparable to the accumulated charge carriers induced by the gate voltage (4.3×10^{12} cm^{-2} at $V_g = 60$ V). This high doping concentration can be the origin of the significant increase of electron mobility in the devices with MAI as it allows a more efficient filling of carrier traps. It is also worth noting that the doping concentration in the TBAI-capped devices is quite close to that obtained in the MAI-capped devices. However, the degree of mobility improvement is remarkably different: in the MAI-capped devices, μ is higher by 1 order of magnitude after BV-doping treatment, whereas it is only a factor of 2 in the TBAI-capped devices. Although the doping concentration is quite close in the devices with both iodide ligands after BV treatment, some remaining oleic acid ligands on the PbS surfaces due to the incomplete removal of

DOI: 10.1021/acsami.7b02867
ACS Appl. Mater. Interfaces 2017, 9, 18039−18045

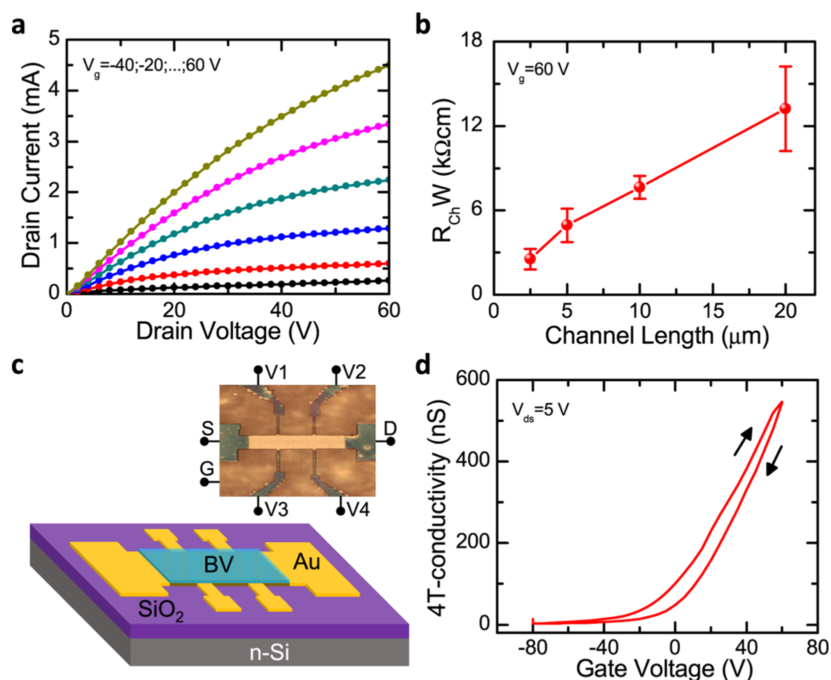

Figure 4. (a) Output characteristics of devices after BV treatment. The range of the applied V_g is between −40 and 60 V (step 20 V). (b) Channel resistances of devices after BV treatment at V_g = 60 V. (c) Device configuration for 4T conductivity measurements. (d) Four-terminal conductivity characteristics of devices after BV treatment (V_{ds} = 5 V).

the native oleic acids with TBAI ligands might suppress the charge transport between neighboring QDs, as previously suggested.[15]

At this point, it is also interesting to measure the contact resistance (R_c) of the devices after BV treatment. Because the devices with MAI ligands show the most efficient n-type doping, we choose these systems for our next investigation. At first sight, we did not observe a contact-limited transport in the output characteristics of the devices at low V_{ds}, as shown in Figure 4a, suggesting low R_c in these devices. To estimate R_c, we fabricated FET devices to apply the transmission-line method with channel lengths of 2.5, 5, 10, and 20 μm. The measured channel resistance, dependent on the channel length, is shown in Figure 4b. R_c is estimated from the intercept of the curve at the y axis (zero channel length). With the BV-doping treatment, the extracted contact resistance (normalized by W; R_cW) of the devices is 0.77 kΩ cm, 1 order of magnitude smaller than that in the pristine devices, as displayed in Figure S3. This low R_c can also have a great impact on the improvement of the charge carrier mobility. It is expected that further improvement of the charge carrier mobility can be achieved by reducing the contact resistance, for instance, by the use of different metals, with shallow work function, for the fabrication of source and drain electrodes.

We then perform 4T conductivity measurements to investigate the charge carrier mobility, μ, in our devices. With these measurements, we are able to exclude the effect of contact resistance, which can limit the charge transport in PbS FETs. The configuration of the devices for 4T conductivity measurements is displayed in Figure 4c. To measure the 4T voltage properly, we perform laser-etching treatment on the PbS films, as displayed in the schematic and photograph in Figure 4c. L and W of the 4T transistor are 150 and 30 μm, respectively. The 4T conductivity in the devices is displayed in Figure 4d and the mobility (μ_{4T}) is calculated using the equation

$$\mu_{4T} = \frac{1}{C_i}\frac{\partial \sigma_{4T}}{\partial V_g} \quad (3)$$

where σ_{4T} is the 4T conductivity. Using eq 3, we obtained the maximum μ_{4T} among the devices with MAI ligands after BV treatment of 0.64 $cm^2\ V^{-1}\ s^{-1}$ (the average mobility = 0.58 $cm^2\ V^{-1}\ s^{-1}$). To our knowledge, this value is the highest among the electron mobilities reported so far in PbS QD-FETs with SiO_2 gate dielectric. Moreover, the high mobility after the BV treatment can be further improved by optimizing the interface quality of the PbS semiconducting films and the gate dielectric, for instance, using hydroxyl-free dielectrics, as in our previous report, opening great opportunities for the fabrication of highly performing solution-processable electronic devices with PbS QDs.[17,39]

■ CONCLUSIONS

In conclusion, we have demonstrated n-type doping of PbS QD-FETs with the use of electron-donating BV molecules. By engineering the LUMO level of the PbS semiconducting films through the use of different capping ligands, we successfully control the electrical characteristics of PbS QD-FETs from ambipolar to heavily n-type. In the devices with MAI ligands, we observe a significant improvement of the electron mobility by more than 1 order of magnitude after the BV-doping treatment. This high mobility is associated with an effective filling of the carrier traps and a reduced contact resistance of the devices. The 4T conductivity transistor measurements reveal mobility as high as 0.64 $cm^2\ V^{-1}\ s^{-1}$ in the devices after BV treatment. These doping results open great opportunities for the exploitation of PbS QDs as n-type materials for broad electronic and optoelectronic applications.

DOI: 10.1021/acsami.7b02867
ACS Appl. Mater. Interfaces 2017, 9, 18039−18045

■ ASSOCIATED CONTENT

Supporting Information

The Supporting Information is available free of charge on the ACS Publications website at DOI: 10.1021/acsami.7b02867.

Hysteresis profiles of the transfer characteristics on the linear and semilogarithmic scale; on-current before and after BV treatment, with given standard deviation; channel resistances of the pristine devices (PDF)

■ AUTHOR INFORMATION

Corresponding Authors

*E-mail: m.a.loi@rug.nl (M.A.L.).
*E-mail: takeya@k.u-tokyo.ac.jp (J.T.).

ORCID

Mohamad Insan Nugraha: 0000-0001-9352-1902
Wolfgang Heiss: 0000-0003-0430-9550

Author Contributions

#M.I.N. and S.K. contributed equally to this work.

Author Contributions

The manuscript was written through contributions of all authors. All authors have given approval to the final version of the manuscript.

Notes

The authors declare no competing financial interest.

■ ACKNOWLEDGMENTS

This work was funded by the University of Groningen and The University of Tokyo. In Groningen, the work was partially supported by the European Research Council (ERC) Starting Grant (No. 306983) "Hybrid solution processable materials for opto-electronic devices" (ERC-HySPOD). W.H. and M.S. gratefully acknowledge the use of the services and facilities of the "Energie Campus Nürnberg" and financial support through the "Aufbruch Bayern" initiative of the State of Bavaria. The authors would like to thank B. Blülle and D.M. Balazs for discussions.

■ REFERENCES

(1) Szendrei, K.; Gomulya, W.; Yarema, M.; Heiss, W.; Loi, M. A. PbS Nanocrystal Solar Cells with High Efficiency and Fill Factor. *Appl. Phys. Lett.* **2010**, *97*, No. 203501.

(2) Piliego, C.; Protesescu, L.; Bisri, S. Z.; Kovalenko, M. V.; Loi, M. A. 5.2% Efficient PbS Nanocrystal Schottky Solar Cells. *Energy Environ. Sci.* **2013**, *6*, 3054−3059.

(3) Chuang, C.-H. M.; Brown, P. R.; Bulović, V.; Bawendi, M. G. Improved Performance and Stability in Quantum Dot Solar Cells through Band Alignment Engineering. *Nat. Mater.* **2014**, *13*, 796−801.

(4) Ip, A. H.; Thon, S. M.; Hoogland, S.; Voznyy, O.; Zhitomirsky, D.; Debnath, R.; Levina, L.; Rollny, L. R.; Carey, G. H.; Fischer, A.; Kemp, K. W.; Kramer, I. J.; Ning, Z.; Labelle, A. J.; Chou, K. W.; Amassian, A.; Sargent, E. H. Hybrid Passivated Colloidal Quantum Dot Solids. *Nat. Nanotechnol.* **2012**, *7*, 577−582.

(5) Oh, S. J.; Berry, N. E.; Choi, J.-H.; Gaulding, E. A.; Paik, T.; Hong, S.-H.; Murray, C. B.; Kagan, C. R. Stoichiometric Control of Lead Chalcogenide Nanocrystal Solids to Enhance Their Electronic and Optoelectronic Device Performance. *ACS Nano* **2013**, *7*, 2413−2421.

(6) Oh, S. J.; Straus, D. B.; Zhao, T.; Choi, J.-H.; Lee, S.-W.; Gaulding, E. A.; Murray, C. B.; Kagan, C. R. Engineering the Surface Chemistry of Lead Chalcogenide Nanocrystal Solids to Enhance Carrier Mobility and Lifetime in Optoelectronic Devices. *Chem. Commun.* **2017**, *53*, 728−731.

(7) Zhao, T.; Goodwin, E. D.; Guo, J.; Wang, H.; Diroll, B. T.; Murray, C. B.; Kagan, C. R. Advanced Architecture for Colloidal PbS Quantum Dot Solar Cells Exploiting a CdSe Quantum Dot Buffer Layer. *ACS Nano* **2016**, *10*, 9267−9273.

(8) Kovalenko, M. V.; Schaller, R. D.; Jarzab, D.; Loi, M. A.; Talapin, D. V. Inorganically Functionalized PbS-CdS Colloidal Nanocrystals: Integration into Amorphous Chalcogenide Glass and Luminescent Properties. *J. Am. Chem. Soc.* **2012**, *134*, 2457−2460.

(9) Pichler, S; Rauch, T; Seyrkammer, R; Böberl, M; Tedde, S. F; Fürst, J; Kovalenko, M. V; Lemmer, U; Hayden, O; Heiss, W Temperature dependent photoresponse from colloidal PbS quantum dot sensitized inorganic/organic hybrid photodiodes. *Appl. Phys. Lett.* **2011**, *98*, No. 053304.

(10) Sukhovatkin, V.; Hinds, S.; Brzozowski, L.; Sargent, E. H. Colloidal Quantum-Dot Photodetectors Exploiting Multiexciton Generation. *Science* **2009**, *324*, 1542−1544.

(11) Szendrei, K.; Cordella, F.; Kovalenko, M. V.; Böberl, M.; Hesser, G.; Yarema, M.; Jarzab, D.; Mikhnenko, O. V.; Gocalinska, A.; Saba, M.; Quochi, F.; Mura, A.; Bongiovanni, G.; Blom, P. W. M.; Heiss, W.; Loi, M. A. Solution-Processable Near-IR Photodetectors Based on Electron Transfer from PbS Nanocrystals to Fullerene Derivatives. *Adv. Mater.* **2009**, *21*, 683−687.

(12) Loi, M. A.; Rost-Bietsch, C.; Murgia, M.; Karg, S.; Riess, W.; Muccini, M. Tuning Optoelectronic Properties of Ambipolar Organic Light-Emitting Transistors Using a Bulk-Heterojunction Approach. *Adv. Funct. Mater.* **2006**, *16*, 41−47.

(13) Schornbaum, J.; Zakharko, Y.; Held, M.; Thiemann, S.; Gannott, F.; Zaumseil, J. Light-Emitting Quantum Dot Transistors: Emission at High Charge Carrier Densities. *Nano Lett.* **2015**, *15*, 1822−1828.

(14) Sun, L.; Choi, J. J.; Stachnik, D.; Bartnik, A. C.; Hyun, B.-R.; Malliaras, G. G.; Hanrath, T.; Wise, F. W. Bright Infrared Quantum-Dot Light-Emitting Diodes through Inter-Dot Spacing Control. *Nat. Nanotechnol.* **2012**, *7*, 369−373.

(15) Balazs, D. M.; Dirin, D. N.; Fang, H.-H.; Protesescu, L.; ten Brink, G. H.; Kooi, B. J.; Kovalenko, M. V.; Loi, M. A. Counterion-Mediated Ligand Exchange for PbS Colloidal Quantum Dot Superlattices. *ACS Nano* **2015**, *9*, 11951−11959.

(16) Kagan, C. R.; Lifshitz, E.; Sargent, E. H.; Talapin, D. V. Building Devices from Colloidal Quantum Dots. *Science* **2016**, *353*, No. aac5523.

(17) Nugraha, M. I.; Häusermann, R.; Bisri, S. Z.; Matsui, H.; Sytnyk, M.; Heiss, W.; Takeya, J.; Loi, M. A. High Mobility and Low Density of Trap States in Dual-Solid-Gated PbS Nanocrystal Field-Effect Transistors. *Adv. Mater.* **2015**, *27*, 2107−2112.

(18) Osedach, T. P.; Zhao, N.; Andrew, T. L.; Brown, P. R.; Wanger, D. D.; Strasfeld, D. B.; Chang, L. Y.; Bawendi, M. G.; Bulović, V. Bias-Stress Effect in 1,2-Ethanedithiol-Treated PbS Quantum Dot Field-Effect Transistors. *ACS Nano* **2012**, *6*, 3121−3127.

(19) Sargent, E. H. Colloidal Quantum Dot Solar Cells. *Nat. Photonics* **2012**, *6*, 133−135.

(20) Yang, J.; Choi, M. K.; Kim, D.-H.; Hyeon, T. Designed Assembly and Integration of Colloidal Nanocrystals for Device Applications. *Adv. Mater.* **2016**, *28*, 1176−1207.

(21) Koh, W.-k.; Saudari, S. R.; Fafarman, A. T.; Kagan, C. R.; Murray, C. B. Thiocyanate-Capped PbS Nanocubes: Ambipolar Transport Enables. *Nano Lett.* **2011**, *11*, 4764−4767.

(22) Oh, S. J.; Berry, N. E.; Choi, J.-H.; Gaulding, E. A.; Lin, H.; Paik, T.; Diroll, B. T.; Muramoto, S.; Murray, C. B.; Kagan, C. R. Designing High-Performance PbS and PbSe Nanocrystal Electronic Devices through Stepwise, Post-Synthesis, Colloidal Atomic Layer Deposition. *Nano Lett.* **2014**, *14*, 1559−1566.

(23) Stinner, F. S.; Lai, Y.; Straus, D. B.; Diroll, B. T.; Kim, D. K.; Murray, C. B.; Kagan, C. R. Flexible, High-Speed CdSe Nanocrystal Integrated Circuits. *Nano Lett.* **2015**, *15*, 7155−7160.

(24) Talapin, D. V.; Lee, J.-S.; Kovalenko, M. V.; Shevchenko, E. V. Prospects of Colloidal Nanocrystals for Electronic and Optoelectronic Applications. *Chem. Rev.* **2010**, *110*, 389−458.

DOI: 10.1021/acsami.7b02867
ACS Appl. Mater. Interfaces 2017, 9, 18039−18045

(25) Talapin, D. V.; Murray, C. B. PbSe Nanocrystal Solids for N- and P-Channel Thin Film Field-Effect Transistors. *Science* **2005**, *310*, 86−89.
(26) Kiriya, D.; Tosun, M.; Zhao, P.; Kang, J. S.; Javey, A. Air-Stable Surface Charge Transfer Doping of MoS_2 by Benzyl Viologen. *J. Am. Chem. Soc.* **2014**, *136*, 7853−7856.
(27) Jang, J.; Liu, W.; Son, J. S.; Talapin, D. V. Temperature-Dependent Hall and Field-Effect Mobility in Strongly Coupled All-Inorganic Nanocrystal Arrays. *Nano Lett.* **2014**, *14*, 653−662.
(28) Ning, Z.; Voznyy, O.; Pan, J.; Hoogland, S.; Adinolfi, V.; Xu, J.; Li, M.; Kirmani, A. R.; Sun, J.; Minor, J.; Kemp, K. W.; Dong, H.; Rollny, L.; Labelle, A.; Carey, G.; Sutherland, B.; Hill, I.; Amassian, A.; Liu, H.; Tang, J.; Bakr, O. M.; Sargent, E. H. Air-Stable N-Type Colloidal Quantum Dot Solids. *Nat. Mater.* **2014**, *13*, 822−828.
(29) Balazs, D. M.; Nugraha, M. I.; Bisri, S. Z.; Sytnyk, M.; Heiss, W.; Loi, M. A. Reducing Charge Trapping in PbS Colloidal Quantum Dot Solids. *Appl. Phys. Lett.* **2014**, *104*, No. 112104.
(30) Klem, E. J. D.; Shukla, H.; Hinds, S.; MacNeil, D. D.; Levina, L.; Sargent, E. H. Impact of Dithiol Treatment and Air Annealing on the Conductivity, Mobility, and Hole Density in PbS Colloidal Quantum Dot Solids. *Appl. Phys. Lett.* **2008**, *92*, No. 212105.
(31) Balazs, D. M.; Bijlsma, K. I.; Fang, H.-H.; Dirin, D. N.; Dobeli, M.; Kovalenko, M. V.; Loi, M. A. Stoichiometric Control of the Density of States in PbS Colloidal Quantum Dot Solids. *Adv. Mater.*, submitted for publication.
(32) Koh, W.-k.; Koposov, A. Y.; Stewart, J. T.; Pal, B. N.; Robel, I.; Pietryga, J. M.; Klimov, V. I. Heavily Doped N-Type PbSe and PbS Nanocrystals Using Ground-State Charge Transfer from Cobaltocene. *Sci. Rep.* **2013**, *3*, No. 2004.
(33) Kim, S. M.; Jang, J. H.; Kim, K. K.; Park, H. K.; Bae, J. J.; Yu, W. J.; Lee, I. H.; Kim, G.; Loc, D. D.; Kim, U. J.; Lee, E.-H.; Shin, H.-J.; Choi, J.-Y.; Lee, Y. H. Reduction-Controlled Viologen in Bisolvent as an Environmentally Stable N-Type Dopant for Carbon Nanotubes. *J. Am. Chem. Soc.* **2009**, *131*, 327−331.
(34) Kim, D. K.; Lai, Y.; Diroll, B. T.; Murray, C. B.; Kagan, C. R. Flexible and Low-Voltage Integrated Circuits Constructed from High-Performance Nanocrystal Transistors. *Nat. Commun.* **2012**, *3*, No. 1216.
(35) Kirmani, A. R.; Kiani, A.; Said, M. M.; Voznyy, O.; Wehbe, N.; Walters, G.; Barlow, S.; Sargent, E. H.; Marder, S. R.; Amassian, A. Remote Molecular Doping of Colloidal Quantum Dot Photovoltaics. *ACS Energy Lett.* **2016**, *1*, 922−930.
(36) Ingram, I. D. V.; Tate, D. J.; Parry, A. V. S.; Sebastian Sprick, R.; Turner, M. L. A Simple Method for Controllable Solution Doping of Complete Polymer Field-Effect Transistors. *Appl. Phys. Lett.* **2014**, *104*, No. 153304.
(37) Lüssem, B.; Tietze, M. L.; Kleemann, H.; Hoßbach, C.; Bartha, J. W.; Zakhidov, A.; Leo, K. Doped Organic Transistors Operating in the Inversion and Depletion Regime. *Nat. Commun.* **2013**, *4*, No. 2775.
(38) Brown, P. R.; Kim, D.; Lunt, R. R.; Zhao, N.; Bawendi, M. G.; Grossman, J. C.; Bulovic, V. Energy Level Modification in Lead Sulfide Quantum Dot Thin Films through Ligand Exchange. *ACS Nano* **2014**, *8*, 5863−5872.
(39) Shulga, A. G.; Piveteau, L.; Bisri, S. Z.; Kovalenko, M. V.; Loi, M. A. Double Gate PbS Quantum Dot Field-Effect Transistors for Tuneable Electrical Characteristics. *Adv. Electron. Mater.* **2016**, *2*, No. 1500467.
(40) Cademartiri, L.; Bertolotti, J.; Sapienza, R.; Wiersma, D. S.; von Freymann, G.; Ozin, G. A. Multigram Scale, Solventless, and Diffusion-Controlled Route to Highly Monodisperse PbS Nanocrystals. *J. Phys. Chem. B* **2006**, *110*, 671−673.
(41) Hines, M. A.; Scholes, G. D. Colloidal PbS Nanocrystals with Size-Tunable Near-Infrared Emission: Observation of Post-Synthesis Self-Narrowing of the Particle Size Distribution. *Adv. Mater.* **2003**, *15*, 1844−1849.